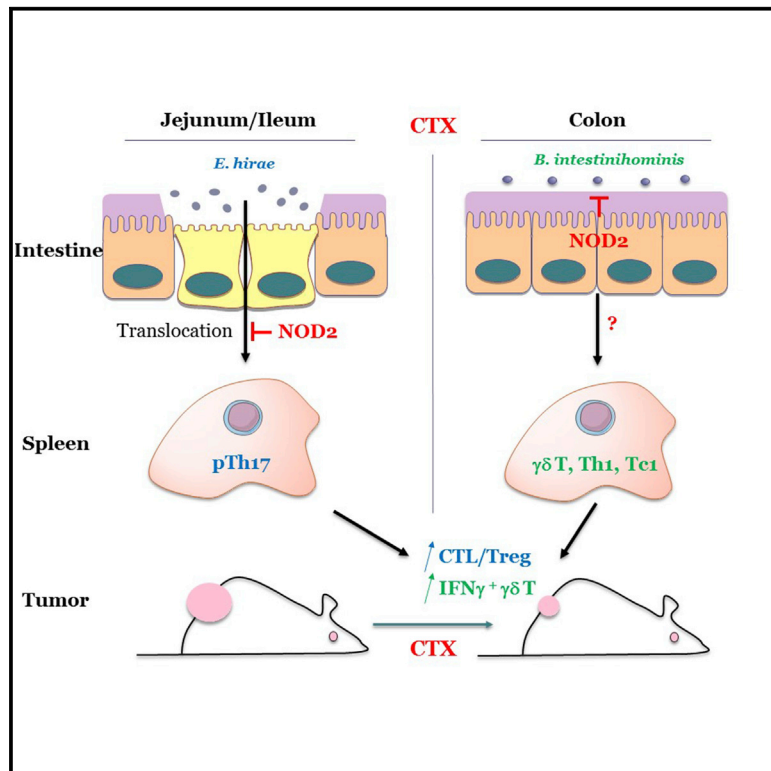Enterococcus hirae and *Barnesiella intestinihominis* Facilitate Cyclophosphamide-Induced Therapeutic Immunomodulatory Effects

Graphical Abstract

Authors

Romain Daillère, Marie Vétizou, Nadine Waldschmitt, ..., Ivo Gomperts Boneca, Mathias Chamaillard, Laurence Zitvogel

Correspondence

laurence.zitvogel@gustaveroussy.fr

In Brief

Cyclophosphamide (CTX) is an immunomodulatory anticancer compound. Daillère et al. show that the antitumoral efficacy of CTX relies on two gut commensal species, *Enterococcus hirae* and *Barnesiella intestinihominis* in a NOD2-dependent manner. These two bacteria changed the tumor microenvironment, reducing regulatory T cells and stimulating cognate antitumor CTL responses.

Highlights

- *E. hirae* restored the efficacy of CTX in antibiotics-treated mice

- *E. hirae* and *B. intestinihominis* enhanced cognate anticancer immune responses

- NOD2 receptors limit the bioactivity of *E. hirae* and *B. intestinihominis*

- CD4+ T cell responses against *E. hirae* are associated with survival in cancer patients

CrossMark

CellPress

Enterococcus hirae and *Barnesiella intestinihominis* Facilitate Cyclophosphamide-Induced Therapeutic Immunomodulatory Effects

Romain Daillère,[1,2,3] Marie Vétizou,[1,2,3] Nadine Waldschmitt,[4] Takahiro Yamazaki,[1,2] Christophe Isnard,[5,6]
Vichnou Poirier-Colame,[1,2,3] Connie P.M. Duong,[1,2,7] Caroline Flament,[1,2,7] Patricia Lepage,[8]
Maria Paula Roberti,[1,2,7] Bertrand Routy,[1,2,3] Nicolas Jacquelot,[1,2,3] Lionel Apetoh,[9,10,11] Sonia Becharef,[1,2,7]
Sylvie Rusakiewicz,[1,2,7] Philippe Langella,[8] Harry Sokol,[8,12,13] Guido Kroemer,[14,15,16,17,18,19] David Enot,[1,15]

(Author list continued on next page)

[1]Institut de Cancérologie Gustave Roussy Cancer Campus (GRCC), 114 rue Edouard Vaillant, Villejuif, 94805, France
[2]Institut National de la Santé Et de la Recherche Medicale (INSERM), U1015, GRCC, Villejuif, 94805, France
[3]University of Paris-Saclay, Kremlin Bicêtre, 94270, France
[4]University Lille, CNRS, Inserm, CHRU Lille, Institut Pasteur de Lille, U1019-UMR 8204-CIIL, Centre d'Infection et d'Immunité de Lille, 59000 Lille, France
[5]Université de Caen Basse-Normandie, EA4655 U2RM (Équipe Antibio-Résistance), Caen, 14033, France
[6]CHU de Caen, Service de Microbiologie, Caen, 14033, France
[7]Center of Clinical Investigations in Biotherapies of Cancer (CICBT) 1428, Villejuif, 94805, France
[8]Micalis Institute, INRA, AgroParisTech, Université Paris-Saclay, 78350 Jouy-en-Josas, France
[9]Lipids, Nutrition, Cancer, INSERM, U866, Dijon, 21078, France
[10]Department of Medicine, Université de Bourgogne Franche-Comté, Dijon, 21078, France
[11]Department of Oncology, Centre Georges François Leclerc, Dijon, 21000, France
[12]AVENIR Team Gut Microbiota and Immunity, ERL, INSERM U 1157/UMR 7203, Faculté de Médecine, Saint-Antoine, Université Pierre et Marie Curie (UPMC), Paris, 75012, France
[13]Service de Gastroentérologie, Hôpital Saint-Antoine, Assistance Publique—Hôpitaux de Paris (APHP), Paris, 75012, France
[14]INSERM U848, 94805 Villejuif, France
[15]Metabolomics Platform, Institut Gustave Roussy, Villejuif, 94805, France
[16]Equipe 11 labellisée Ligue contre le Cancer, Centre de Recherche des Cordeliers, INSERM U 1138, Paris, 75006, France
[17]Pôle de Biologie, Hôpital Européen Georges Pompidou, AP-HP, Paris, 75015, France
[18]Université Paris Descartes, Sorbonne Paris Cité, Paris, 75006, France
[19]Karolinska Institute, Department of Women's and Children's Health, Karolinska University Hospital, Stockholm, 17176, Sweden
[20]INSERM U970, Paris Cardiovascular Research Center, Université Paris-Descartes, Sorbonne Paris Cité, Paris, 75015, France
[21]Service d'immunologie biologique, Hôpital Européen Georges Pompidou, Paris, 75015 France
[22]INSERM U1143, 75005 Paris, France
[23]Institut Curie, PSL Research University, Endocytic Trafficking and Therapeutic Delivery group, Paris, 75248, France
[24]CNRS UMR 3666, Paris, 75005, France

(Affiliations continued on next page)

SUMMARY

The efficacy of the anti-cancer immunomodulatory agent cyclophosphamide (CTX) relies on intestinal bacteria. How and which relevant bacterial species are involved in tumor immunosurveillance, and their mechanism of action are unclear. Here, we identified two bacterial species, *Enterococcus hirae* and *Barnesiella intestinihominis* that are involved during CTX therapy. Whereas *E. hirae* translocated from the small intestine to secondary lymphoid organs and increased the intratumoral CD8/Treg ratio, *B. intestinihominis* accumulated in the colon and promoted the infiltration of IFN-γ-producing $\gamma\delta$T cells in cancer lesions. The immune sensor, NOD2, limited CTX-induced cancer immunosurveillance and the

bioactivity of these microbes. Finally, *E. hirae* and *B. intestinihominis* specific-memory Th1 cell immune responses selectively predicted longer progression-free survival in advanced lung and ovarian cancer patients treated with chemo-immunotherapy. Altogether, *E. hirae* and *B. intestinihominis* represent valuable "oncomicrobiotics" ameliorating the efficacy of the most common alkylating immunomodulatory compound.

INTRODUCTION

Cancer results from a complex interplay between gene regulation and its environment. Microbial communities inhabiting our intestine and other portals of entry represent unappreciated

Antoine Roux,[1,2,3,18] Alexander Eggermont,[1,3] Eric Tartour,[20,21] Ludger Johannes,[22,23,24] Paul-Louis Woerther,[25] Elisabeth Chachaty,[25] Jean-Charles Soria,[1,3] Encouse Golden,[26] Silvia Formenti,[26] Magdalena Plebanski,[27] Mutsa Madondo,[27] Philip Rosenstiel,[28] Didier Raoult,[29] Vincent Cattoir,[5,6,30] Ivo Gomperts Boneca,[31] Mathias Chamaillard,[4] and Laurence Zitvogel[1,2,3,7,32],*

[25]Service de microbiologie, GRCC, Villejuif, 94805, France

[26]Department of Radiation Oncology, Weill Cornell Medicine, New York, NY, USA

[27]Department of Immunology and Pathology, Monash University, Alfred Hospital Precinct, Melbourne, Prahran, Victoria 3181, Australia

[28]Institute of Clinical Molecular Biology, Christian-Albrechts-University and University Hospital Schleswig-Holstein, Campus Kiel, 24105 Kiel, Germany

[29]AIX MARSEILLE UNIVERSITE, URMITE (Unité de Recherche sur les Maladies Infectieuses et Tropicales Emergentes), UMR 7278, INSERM 1095, IRD 198, Faculté de Médecine, Marseille 13005, France

[30]CNR de la Résistance aux Antibiotiques, Laboratoire Associé Entérocoques, Caen, 14033, France

[31]Institut Pasteur, Unit Biology and Genetics of the bacterial Cell Wall, Paris, 75015, France

[32]Lead author

*Correspondence: laurence.zitvogel@gustaveroussy.fr

http://dx.doi.org/10.1016/j.immuni.2016.09.009

environmental factors that appear to play a role in intestinal and extraintestinal carcinogenesis (Zitvogel et al., 2015). Pioneering studies performed in germ-free and gnotobiotic animals or in antibiotic-treated rodents revealed an unsuspected role of commensals in tumorigenesis. In the colon cancer or hepatocarcinoma, microbes can directly be transforming agents (Sears and Garrett, 2014) by providing a toxic metabolite, an oncogenic product or inducing an inflammatory milieu which will culminate in genomic instability and/or DNA damage responses and/or immune escape (Gur et al., 2015; Louis et al., 2014). A role for Toll-like receptor 5-dependent commensal microbes in interleukin-6 (IL-6) or IL-17–driven systemic inflammation was demonstrated in extraintestinal neoplasia (Rutkowski et al., 2015). In contrast, other observations support a beneficial role of distinct bacteria against cancer. Prolonged exposure to a combination of metronidazole and ciprofloxacine tripled breast cancer (BC) occurrence in protooncogene HER2/neu driven-transgenic mice (Rossini et al., 2006). In humans, epidemiological studies suggested a dose-dependent association between antibiotic use and risk of BC (Blaser, 2011; Velicer et al., 2004). The beneficial role of the intestinal microbiota was first reported by Paulos et al. showing that total body irradiation promoted a LPS-TLR4-dependent activation of antigen-presenting cells facilitating the efficacy of adoptive T cell transfer (Paulos et al., 2007). Next, Iida et al. reported that bacteria-associated TLR4 agonists accounted for the ROS and TNF-α-mediated antitumor effects of tumor infiltrating myeloid cells (MDSC) during platinum-based anticancer therapies and immunomodulatory regimen (Iida et al., 2013). We also showed that cyclophosphamide (CTX) promoted the translocation of distinct Gram+ bacteria (mainly Lactobacillus johnsonii and Enterococcus hirae) that mounted effector pathogenic Th17 (pTh17) cell responses associated with tumor control (Viaud et al., 2013). We and others showed that distinct intestinal bacterial species belonging to Bacteroidales and Burkholderiales or Bifidobacteriales orders influenced the tumor microenvironment, contributing to the efficacy of anti-CTLA4 or anti-PDL-1 Ab, respectively (Vétizou et al., 2015; Sivan et al., 2015).

Hence, the intestinal microbiota ecosystem might control not only the gut immune homeostasis but also the inflammatory and/or immune tone of secondary lymphoid organs, culminating in shaping the tumor microenvironment. This hypothesis implies that anticancer therapeutics alter the delicate mutualistic symbiosis between intestinal epithelial cells, the local microbiome, and the lamina propria resident-immune system, contributing to reprogram anticancer immune responses. The precise identification of bacterial genera capable of linking intestinal and anti-cancer immune responses is key to the emerging field of "oncomicrobiotics" (OMBs), i.e., immunogenic commensals influencing the host-cancer equilibrium.

Here, we identified two intestinal OMBs, namely E. hirae and Barnesiella intestinihominis, that both act to orchestrate the anticancer therapeutic effects of CTX. The small intestine-resident Gram+ bacteria E. hirae induces systemic pTh17 cell responses associated with tumor antigen-specific, MHC class I-restricted cytotoxic T cells (CTL) and increased intratumoral CTL/T regulatory (Treg) cell ratio. The colon resident Gram− B. intestinihominis boosts systemic polyfunctional Tc1 and Th1 cell responses and reinstate intratumoral IFN-γ producing γδT cells. Both commensals reduced Treg cells in the tumor microenvironment (Foxp3 and/or γδT17 cells). These two immunogenic commensals are kept in check by intestinal NOD2 receptors, limiting their direct proapoptotic effects on epithelial cells and their accumulation in vivo. Memory Th1 immune responses toward E. hirae or B. intestinihominis are clinically relevant, dictating progression-free survival (PFS) in end-stage cancer patients.

RESULTS

E. hirae Restored the Efficacy of CTX in Antibiotics-Treated Mice

We previously reported that broad spectrum antibiotics (ATBs) and vancomycin decreased the anticancer activity of CTX in vivo. We then showed that CTX compromised the integrity of the intestinal epithelium, promoting the translocation of distinct Gram+ bacteria in secondary lymphoid organs that could elicit L. johnsonii or E. hirae specific Th1 cell responses (Viaud et al., 2013). However, we did not demonstrate the causal relationship between the translocating Gram+ bacteria and the CTX-induced tumoricidal activity.

To analyze the antitumor effects of those Gram+ bacterial species capable of translocating to secondary lymphoid organs post-CTX, we performed a gut colonization of mouse intestines with 10^9 E. hirae (clone 13144), L. johnsonii or control bacteria
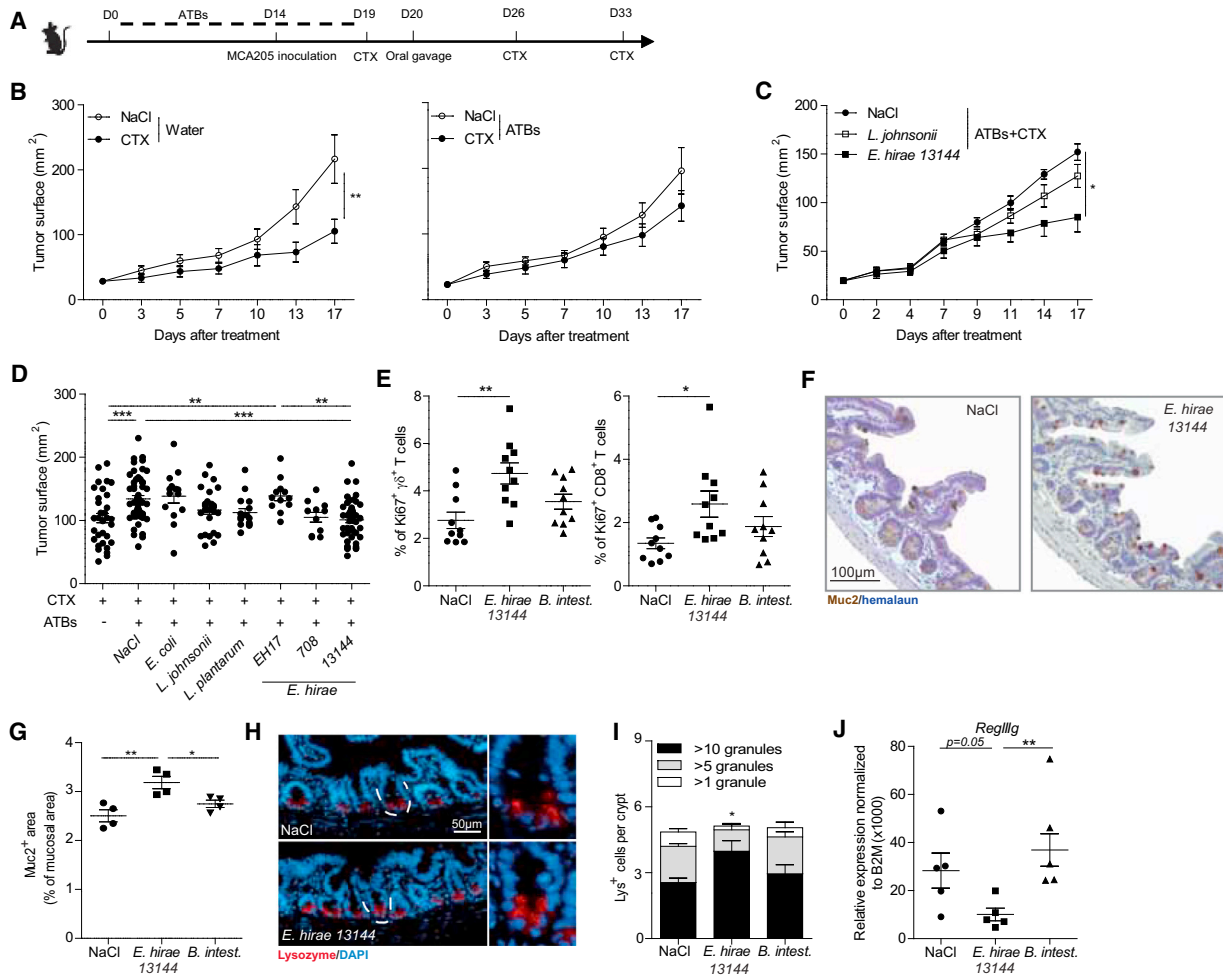
Figure 1. The Oncobiotic *E. hirae* Boosts CTX Efficacy in ATBs-Induced Dysbiosis

(A) Experimental setting.

(B–D) OMB effects of *E. hirae*. Tumor growth kinetics with or without ATBs (B) and after oral gavage *E. hirae*, *L. johnsonii* (C), or other bacterial species (D). Day 0 in B represents day 19 in (A). A typical growth curve is depicted for five mice per group (B and C) and tumor sizes at day 19 post-CTX are pooled for 2–4 experiments containing at least five mice per group (D).

(E) Proliferation of intraepithelial lymphocytes of the small intestine 2 days after oral gavage assessed by flow cytometry. Each dot represents one mouse intestine

(F and G). Hyperplasia of goblet cells 4 days after oral gavage with *E. hirae* assessed by immunohistochemistry staining. One micrograph picture is representative of a control and *E. hirae*-treated mice. The graph depicts the area of positive cells/mucosal area (one dot per mouse) (H–I). Lysozyme containing Paneth cells at the bottom of the crypts in the jejunum. One micrograph picture is representative of a control and *E. hirae*-treated mice at two different magnifications. Enumeration of positive cells/crypt with different amounts of granules in three categories in four mice per group (means ± SEM for a minimum of 10 crypts).

(J) Transcription levels of the antimicrobial peptide RegIIIγ assessed by qPCR of the intestinal mucosae 2 days after oral gavage. Statistical analyses were performed by a linear mixed-effects modeling (B and C), Dunnett (D, E, and G) and Mann-Whitney (I and J) tests. All data are expressed as mean ± SEM: *$p < 0.05$, **$p < 0.01$, ***$p < 0.001$. B. intest, *Barnesiella intestinihominis*. Related to Figure S1.

in MCA205 sarcoma-bearing mice rendered dysbiotic by a 14 day-broad spectrum ATBs regimen (Figure 1A). Broad spectrum ATBs prevented the metronomic CTX-mediated control of tumor growth (Figure 1B). However, oral gavage with *E. hirae* clone 13144 selectively restored the CTX-mediated antitumor effects whereas our *L. johnsonii*, *E. coli*, or *Lactobacilli* isolates failed to do so (Figures 1C and 1D).

To assess the effective colonization by *E. hirae*, we performed ex vivo cultivation of feces on agar plates (followed by mass spectrometry identification of bacteria), qPCR with enterococci-specific probes, and FISH analyses of mucosal and luminal compartments at various locations of the small and large intestine. These assays concluded that by 24 hr post-gavage, all detectable bacteria were *E. hirae*, which were very abundant in the jejunum and ileum and were not only present in the lumen but also in the mucosa for at least 4 days (Figures S1A–S1D). Additionally, supplementation with *E. hirae* (and not colonization with a Gram- bacteria residing in the colon such as *B. intestinihominis*) induced the proliferation of γδT cells and CD8+ T cells residing in the epithelial layer (Figure 1E), as well as an hyperplasia of mucin-producing goblet cells (Figures 1F and 1G) and lysozyme-containing Paneth cells
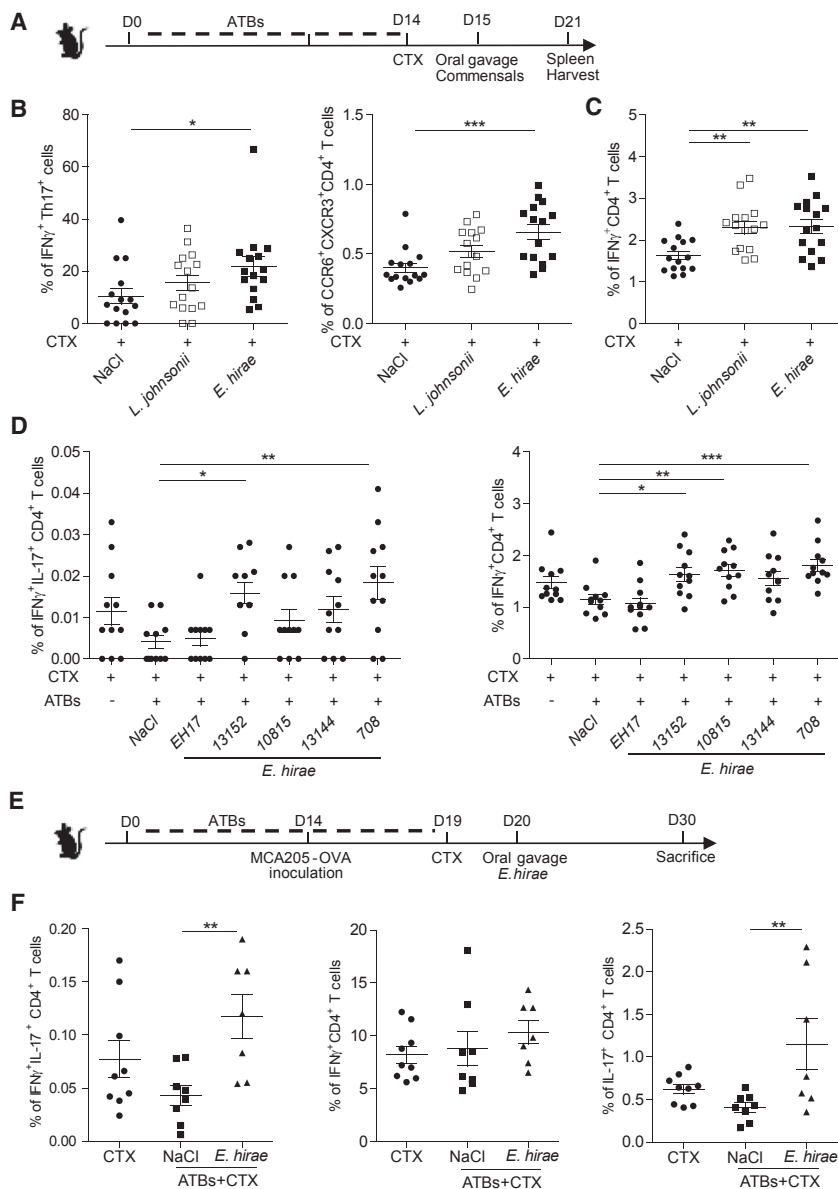
Figure 2. Immunomodulatory Effects of *E. hirae* in Naive and Tumor Bearers

(A) Experimental setting.

(B and C). Flow cytometric analyses of Th1 and pTh17 cells after oral gavage with various commensals (including *E. hirae 13144*). CD4$^+$ T cells expressing or co-expressing IFN-γ and/or IL-17 (B and C) or CXCR3 and CCR6 (B, right panel) in the gate of live CD3$^+$ splenocytes.

(D) Effects of five different isolates of *E. hirae* shown for two independent experiments in naive mice.

(E and F) Experimental setting in tumor bearers (E). Flow cytometric immunomonitoring of pTh17 (left panel), Th1 (middle panel), and Th17 (right panel) (F). Two experiments are depicted with data expressed as mean ± SEM. Statistical analyses were performed by a Dunnett test:*p < 0.05, **p < 0.01, ***p < 0.001. Related to Figures S2 and S3 and Table S1.

We tested various *E. hirae* isolates derived from human, mouse, or environmental ecosystems to analyze their differential immunogenicity in vivo and their capacity to mediate "oncomicrobiotic" property. These strains, which were equally susceptible to antimicrobial agents (Table S1), failed to produce virulence gene products (such as *cob*, *cylA*, *efaA*$_{efm}$, *efaA*$_{efs}$, *cpd*, *cylB*, *ccf*, *gel*, *esp*, *agg*, *cylM*, *copZ*) as opposed to pathogenic *Enterococcus faecalis.* Of note, *E. hirae 13144* (the isolate we cultivated from mouse spleens post-CTX) failed to exhibit virulence in the in vivo infection model *Galleria mellonella* (Figure S2D). The investigation of clonal relationship between these *E. hirae* isolates by rep-PCR revealed an important genomic diversity within these strains (Figure S2C). Half of the isolates induced pTh17 and Th1 immune responses (Figure 2D) with only one human isolate (clone 708) exhibiting Tc1 potential in naive mice associated with OMB properties (Figure 1D, data not shown). The only human isolate of *E. hirae* (clone EH17) capable of forming ex vivo biofilms on adherence assays harbored no immunogenic nor OMB properties (Figures 1D and 2D and S2E). We next re-examined these immunogenic properties in the setting of a growing sarcoma MCA205 known to influence the gut microbiome (Viaud et al., 2013) (Figure 2E). In tumor bearers, *E. hirae* 13144 induced Th17 and pTh17 but not Th1 immune responses (Figure 2F), suggesting that inflammatory cytokines (such as TGF-β, IL-6, IL-1β, IL-23) involved in pTh17 cell differentiation may fluctuate with the tumor bulk. Of note, the poorly immunogenic *E. hirae* clone EH17 did not induce high IL-1β secretion levels from dendritic cells ex vivo (as opposed to clone 13144 or clone 708) (Figure S3).

Thus, *E. hirae* exerts a capacity to induce pTh17 cells in secondary lymphoid organs of CTX-treated and dysbiotic animals, associated with its OMBs properties.

(Figures 1H and 1I) associated with a slight reduction of the antimicrobial peptide RegIIIγ (Figure 1J).

We next analyzed the immunological effects of *E. hirae* in the secondary lymphoid organs of naive animals. Six days after bacterial colonization, we harvested splenocytes to perform a flow cytometric analyses focusing on IFN-γ^+ and/or IL-17$^+$, as well as CXCR3$^+$ and/or CCR6$^+$ T cells (Figure 2A). In naive mice, *E. hirae* failed to give rise to CD3$^+$CD4$^+$IL-17$^+$ or CCR6$^+$ T cells (called Th17 cells, data not shown) but selectively mounted pTh17 immune responses characterized by the splenic accumulation of rare double positive IFN-γ^+IL-17$^+$ cells or CCR6$^+$ CXCR3$^+$CD4$^+$ T cells (Figure 2B) eventually leading to the differentiation of bona fide CD3$^+$CD4$^+$IFN-γ^+ or CXCR3$^+$ T cells (called Th1 cells, Figures 2C and S2A), polarization corroborated by cell sorting and qPCR detecting *Tbx21* and *Il21* gene expression (Figure S2B).
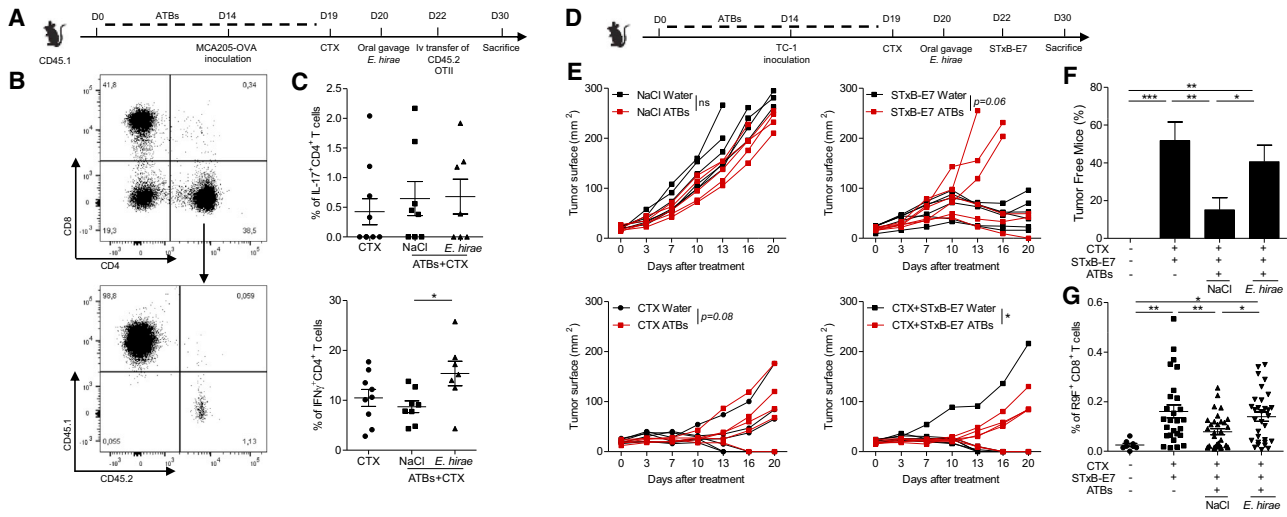
Figure 3. *E. hirae* Induces Tumor Antigen-Specific Cognate T Cell Responses

(A) Experimental setting. Adoptive transfer of CD45.2+ OTII transgenic CD4+ T cells into CD45.1+ hosts bearing OVA-expressing sarcomas and subjected to oral gavage with NaCl or *E. hirae*.

(B and C) Percentages of Th1 and Th17 cells in tumor bearers post-CTX with or without ATBs by flow cytometry. A representative dot plot gating on CD45.2+CD4+ T cells for the intracellular staining is shown. Pooled data from two independent experiments are shown, each dot representing one mouse.

(D–F) Experimental setting with HPV16-E7 expressing TC1 tumors. Tumor growth curves with or without ATBs (E) in a representative experiment out of two. Percentages of complete tumor eradication (F) and monitoring of the proportions of $D^b_{-E739-47}$ tetramer binding CD8+ T cells in the spleens at sacrifice (five concatanated experiments, each dot representing one mouse).

(G). Statistical analyses were performed by Dunnett test (C and G), linear mixed-effects modeling (E), and Firth's penalized-likelihood logistic regression modeling (F). All data are expressed as mean ± SEM: *p < 0.05, **p < 0.01, ***p < 0.001.

E. hirae Enhanced Cognate Anticancer Immune Responses

To investigate whether *E. hirae*-associated systemic immune responses could promote anti-tumor cognate T cell responses, we set up two distinct preclinical models. First, tumor cell lines genetically modified to express the ovalbumine antigen (OVA) were implanted subcutaneously (s.c.) following a 14-day-broad spectrum ATBs therapy. Then, animals were adoptively transferred with $OVA_{323-339}$ specific MHC class II-restricted OTII TCR transgenic T cells and treated with CTX (Figure 3A). We monitored the immunological impact of an oral gavage with *E. hirae* on the activation of congenic CD45.2+ OTII cells in the spleen. In contrast to syngenic CD45.1+ T cells, which differentiated into Th17 cells (Figure 2E), OTII transgenic T were geared toward Th1 cells following colonization with *E. hirae* 13144 (Figures 3B and 3C). Next, we used a s.c. TC1 model expressing the human papillomavirus 16 (HPV16) E7 (Vingert et al., 2006) in which tumor regression could be obtained by vaccinating mice using a non-replicative delivery system composed of the B subunit of Shiga toxin coupled to E7 antigen (STxB-E7) (Figure 3D). This immunization protocol elicited polyfunctional D^b-E7$_{39-47}$ tetramer binding CD8+T cells (Sandoval et al., 2013). Interestingly, the combination of STxB-E7 and CTX ("vaccine") was synergistic, eventually leading to complete tumor eradication (Figure 3E). Here again, a negative impact of broad spectrum ATBs on the efficacy of the "vaccine" was observed with a marked reduction of complete tumor rejection rates in ATBs-compared with water-treated groups (Figures 3E and 3F). Next, we monitored the impact of an oral gavage with *E. hirae* on the probability of complete cure and on the expansion of

polyfunctional D^b-E7$_{39-47}$ tetramer binding CD8+ T cells in the spleens post-ATBs. Indeed, *E. hirae* compensated the lack of efficacy of the cancer "vaccine" in ATBs-treated mice (Figure 3F) with or without the use of STxB-E7 (data not shown) and restored, in ATBs-treated mice, the expansion of D^b-E7$_{39-47}$ tetramer binding CD8+ T cells observed in naive mice CTX-treated positive controls (Figure 3G). Thus, mono-association of "gut sterilized" mice with *E. hirae* could partially restore CTX-induced anticancer Th1 cell or CTL responses, keeping in check tumor progression.

Porphyromonadaceae Family Members (genus *Barnesiella*) Are Involved in the Long-Term Immunogenicity of CTX

We previously showed that CTX could induce Gram+ bacteria translocation (Viaud et al., 2013). To analyze the potential impact of the major pattern-recognition receptors in Gram+ bacterial translocation to the mesenteric LN or spleen, we screened Myd88-, TLR2-, TLR4-, TLR2xTLR4-, and NOD1xNOD2-deficient mice for the presence of cultivatable commensals in secondary lymphoid organs at 48 hr post-CTX. We found a significant increase of bacterial translocation in these $Nod1^{-/-}Nod2^{-/-}$ mice (Figure 4A and data not shown). We next monitored tumor growth kinetics in MCA205-bearing WT versus $Nod1^{-/-}Nod2^{-/-}$ C57BL/6 mice. The CTX antitumor efficacy was markedly enhanced in $Nod1^{-/-}Nod2^{-/-}$ hosts compared with age matched controls bred in the same animal facility (Figure 4B). We phenocopied these effects using pharmacomimetics, i.e., agonists for NOD1 and NOD2 receptors, namely the peptidoglycans MurNAc-L-Ala-γ-D-Glu-mDAP
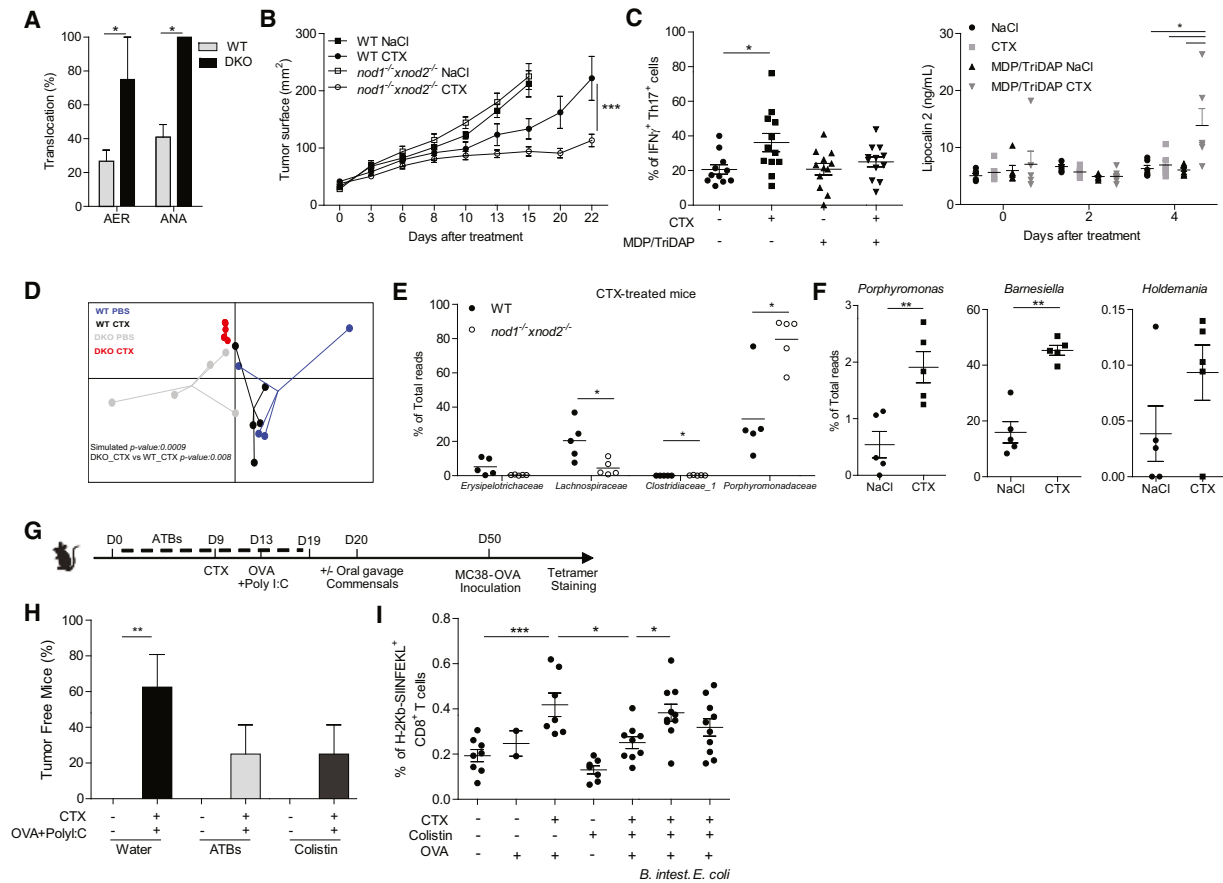
Figure 4. NOD-Dependent *Barnesiella* Accumulation and CTX-Induced Long Term Memory Tc1 Responses

(A) CTX-induced translocation of bacteria in WT versus *Nod1−/−Nod2−/−* (DKO) mice. Naive mice were treated with one i.p. injection of CTX 100 mg/kg and mLN were cultivated on agar plates in aerobic (AER) or anaerobic (ANA) conditions 48 hr later (followed by mass spectrometry identifying *E. hirae*, *L. johnsonii*, or *L. reuteri*). The percentages of positive plates are depicted for two independent experiments.

(B) Tumor growth curves after administration of CTX in WT versus DKO mice. One representative experiment out of two is depicted.

(C) Flow cytometric analyses of splenic CD4+ T cells co-expressing IFN-γ in the gate of live IL-17+ T splenocytes in WT mice treated with systemic daily administration of NOD agonists. Concatenated data of two experiments are shown, one dot representing one mouse (C, left panel). ELISA monitoring of lipocalin-2 in the feces of mice treated with CTX±NOD agonists (C, right panel).

(D) Principle component analyses of the fecal microbiota of CTX-treated WT mice versus their *DKO* littermates. Feces have been harvested at day 7 post-CTX in 5 naive C57BL/6 mice.

(E) Details of the bacterial families residing in feces significantly under- or overrepresented in CTX treated groups comparing WT versus DKO mice.

(F) Analyses of most significant variations of the family members induced by CTX in DKO animals.

(G) Experimental setting. The percentages of tumor-free mice were scored for two experiments (H). The percentages of H-2b-SIINFEKL tetramer-binding CD8+ T cells are indicated for each mouse in three individual experiments (I). Statistical analyses were performed by a linear mixed-effects modeling (B), Firth's penalized-likelihood logistic regression modeling (A and H), Dunnett (C and I), and Mann-Whitney (D–F) tests. All data are expressed as mean ± SEM: *p < 0.05, **p < 0.01, ***p < 0.001. B. intest, *Barnesiella intestinihominis*. Related to Figure S4 and Table S2.

(TriDAP) and muramyl dipeptide in WT mice, respectively. These compounds reduced CTX-mediated pTh17 cells in the spleen (Figure 4C, left panel). This was found to be associated with increased intestinal release of the antimicrobial peptide lipocalin-2 in stools that might in turn facilitate epithelial repair and reduction of intestinal permeability (Figure 4C, right panel).

Consequently, we performed pyrosequencing analyses of 16S rRNA gene amplicons from both the mucosa of the small intestine and stools harvested from naive WT mice versus their *Nod1−/−Nod2−/−* littermates 7 days post-CTX. Principle component analyses revealed that bacterial community structures were significantly different between CTX groups from WT versus gene

deficient mice for the families and genera at both locations (Figures 4D, S4, and Table S2 for the OTU). There was an overrepresentation of *Clostridiaceae* in the small intestines (Figure S4C), mainly attributable to segmented filamentous bacteria (Table S2) and of the *Porphyromonadaceae* family (mainly genus *Barnesiella*) and genus *Holdemania* in the stools. Moreover, there was a relative loss of *Erysipelotrichaceae* in the small intestine as well as *Lachnospiraceae* in feces of *Nod1−/−Nod2−/−* naive mice receiving CTX compared with PBS (Figures 4E and 4F and S4).

The antitumor effects mediated by CTX were compromised in the presence of colistin, an antibiotic regimen killing mainly Gram− bacteria (Viaud et al., 2013). Taking into account the
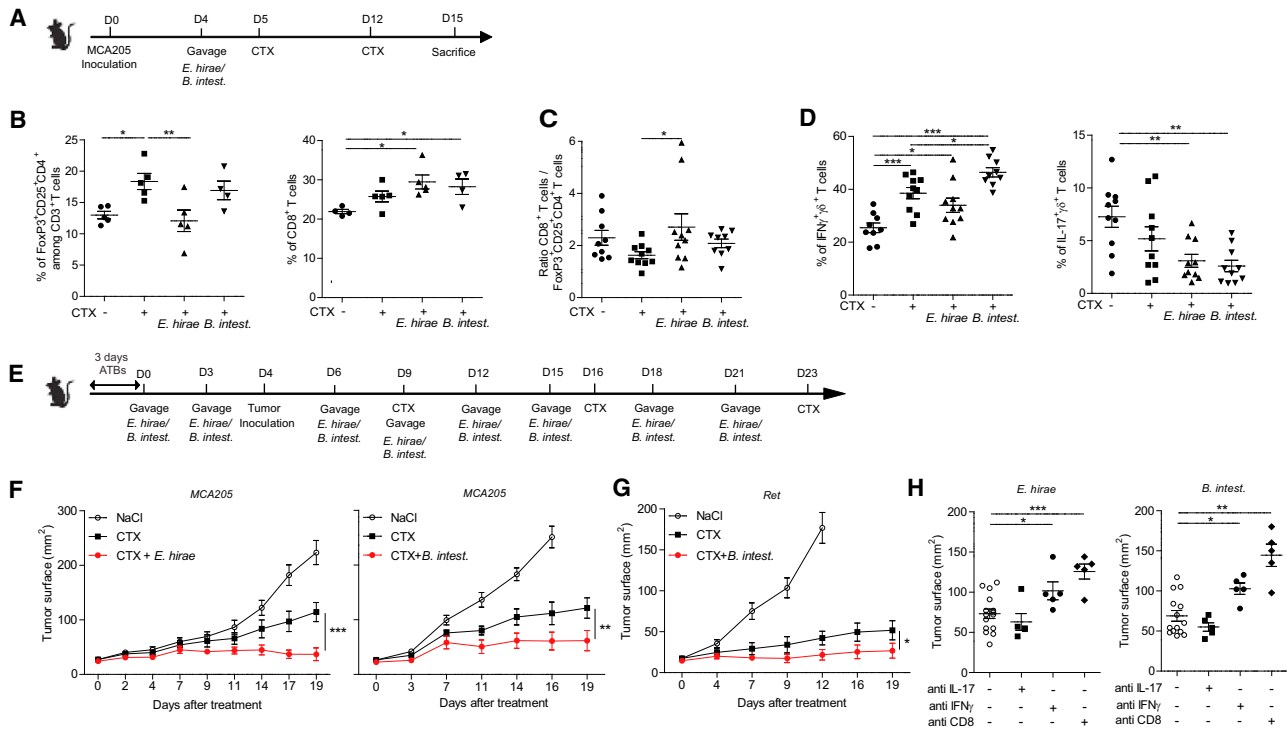
Figure 5. OMBs modulate the tumor microenvironment in the context of CTX in the absence of ATBs

(A–E) Experimental settings. Administration of OMBs in tumor bearers in once in the absence of ATBs (A) and in a repetitive manner after three days of ATBs (E).

(B–D) Flow cytometry analyses of TIL infiltrates, gating on Foxp3+CD25+ CD4+ T cells (Treg) and CD8+ T cells (B), allowing to calculate the ratio between CD8+ T/Treg (C), as well as of IFN-γ or IL-17 producing γδT cells (D).

(F and G) Influence of iterative gavages of OMBs on the CTX-mediated tumor growth curves against MCA205 (F) and Ret melanoma (G) in a representative experiment out of two yielding similar results.

(H) Effects of neutralizing anti-IFN-γ, IL-17, or depleting anti-CD8 antibodies on the antitumor effects of OMBs. Statistical analyses were performed by Dunnett (B and D) and Mann-Whitney (C and H) tests, as well as a linear mixed-effects modeling (F and G). All data are expressed as mean ± SEM: *p < 0.05, **p < 0.01, ***p < 0.001. B. intest, *Barnesiella intestinihominis*. Related to Figure S5.

overrepresentation of Gram⁻ genera isolated in $Nod1^{-/-}Nod2^{-/-}$ mice exhibiting a superior anticancer response to CTX than WT mice, we addressed the role of Gram⁻ bacteria in the adjuvant effect of CTX in the context of a vaccine comprising a cognate cancer antigen, such as the OVA+polyI:C-based cancer immunization procedure (Figure 4G). Indeed, broad spectrum ATBs, as well as colistin, prevented the long-term protection of this cancer vaccine against the lethal challenge with OVA-engineered MC38 tumor cells (Figure 4H). Moreover, colistin prevented the elicitation of H-2K^b/SIINFEKL-restricted CD8+ CTL responses (Figure 4I). To scrutinize which Gram⁻ gut adjuvants could possibly be involved in CTX-induced long term cognate immune responses, we performed an oral gavage with two Gram⁻ species (either *B. intestinihominis* or *E. coli*) after conditioning with colistin during the immunization schedule (Figure 4G). *B. intestinihominis* was selectively capable of restoring H-2K^b/SIINFEKL-restricted CD8+ CTL responses in colistin-treated mice that received the CTX-based vaccine (Figure 4I).

Altogether, distinct *Porphyromonadaceae* family members (genus *Barnesiella*) were overrepresented in the large intestine of CTX-treated mice in conditions of NOD1 and NOD2 functional deficiencies, which might be relevant to account for long-term memory Tc1 cell immune responses protective against tumor establishment.

Considering that two commensals, *E. hirae* or *B. intestinihominis*, appeared regulated either by translocation or accumulation in feces immediately after CTX administration, we next addressed whether they could modulate systemic and local tumor immunity in the absence of ATBs-induced dysbiosis (Figure 5A). Both OMBs induced an inversion of the CD4/CD8 T cell ratio in the spleen, facilitating the accumulation of effector CD8+ T cells (Figures S5A and 5B). Whereas *E. hirae* maintained its capacity to induce pTh17 in the spleen in the absence of ATBs (Figure S5C), *B. intestinihominis* induced polyfunctional CD4+ Th1 and CD8+ Tc1 cells (Figure S5D). Importantly, *E. hirae* markedly reduced the numbers of regulatory Foxp3+CD25+CD4+ tumor infiltrating lymphocytes (TILs), increasing the CTL/Treg cell ratio (Figures 5B and 5C), whereas *B. intestinihominis* augmented the proportions of IFN-γ-producing γδTILs while decreasing IL-17-producing γδTILs, the latter phenomenon being also observed with the other OMBs (Figure 5D).

Repetitive gavages of either OMBs (Figure 5E) were markedly effective in ameliorating the CTX activity against MCA205 fibrosarcoma (Figure 5F). Interestingly, gavages with *B. intestinihominis* was also effective against Ret melanoma (Figure 5G). Of note, in the absence of CTX, *E. hirae* was not able to impact the natural tumor growth of MCA205 sarcoma (Figures S5E and S5F). The neutralization of IFN-γ (but not that of IL-17) or the depletion of
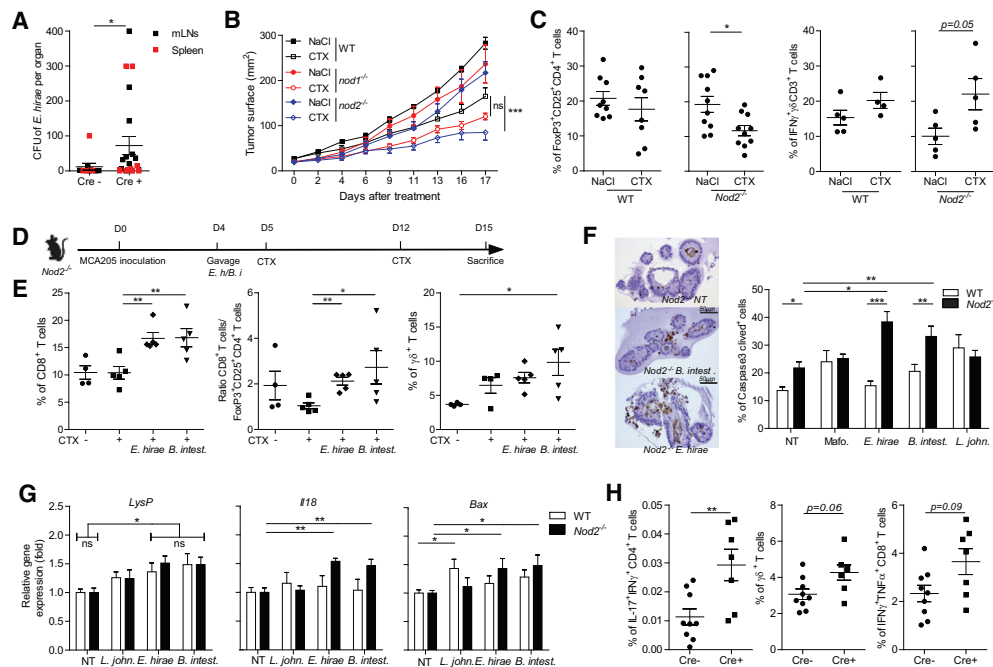
Figure 6. NOD2 Is a Gut Immune Checkpoint Limiting the Biological Effects of OMBs

(A) Villin-driven NOD2 deficiency induced increased translocation of *E. hirae*. *Nod2*$^{fl/fl}$; villin-Cre$^+$ and Cre$^-$ conditional mice were treated with tamoxifen and were orally gavaged with *E. hirae* prior to and right after 100 mg/kg of CTX ip. Mesenteric LN or spleen were cultivated 48 hr later as in Figure 4A. The number of colonies identified by mass spectrometry as being *E. hirae* per plate are depicted (Cre$^+$ versus Cre$^-$). Of note, there was also an increase of the percentages of positive plates (data not shown).

(B). Tumor growth curves after administration of CTX (as in Figure 4B) in WT versus *Nod1*$^{-/-}$ or *Nod2*$^{-/-}$ single KO mice. One representative experiment out of two is depicted (B).

(C). Flow cytometric determination of TIL infiltrates in WT versus *Nod2*$^{-/-}$ genetic strains at day 10 post-CTX.

(D and E) Administration of OMBs by gavage before metronomic CTX to treat MCA205 in *Nod2*$^{-/-}$ mice in the absence of ATBs to examine the effects of OMBs on the tumor microenvironment by flow cytometry. One representative experiment is depicted.

(F and G) WT versus *Nod2*$^{-/-}$ crypt-derived 3D small intestine enteroids exposed to mafosfamide or various commensal bacteria, examined by immunohistochemistry using anti-cleaved caspase-3 Ab (F). Percentages of apoptotic IECs in > 10 enteroids examined per condition. (G) Transcriptional levels by qPCR of Lysozyme P, *Il18*, and Bax gene products in the same enteroids.

(H) Immunological effects of CTX in *Nod2*$^{fl/fl}$; villin-Cre$^+$ and *Nod2*$^{fl/fl}$; villin Cre$^-$ IECs. Statistical analyses were performed by a linear mixed-effects modeling (B), Mann-Whitney (A, C, G, and H), and Dunnett (E and F) tests. All data are expressed as mean ± SEM: *p < 0.05, **p < 0.01, ***p < 0.001. Related to Figure S6.

CD8$^+$ T cells using systemic injections of antibodies severely impaired the anticancer efficacy of OMBs against MCA205 (Figure 5H). Thus, these two commensal bacteria have an adjuvant impact on systemic and tumoral immune responses immunomodulated by metronomic CTX.

NOD2 as an Epithelial-Operating Immune Checkpoint for the Adjuvant Effects of OMBs Independently of Ripk2 and Card9

Intrigued by the exacerbated Gram$^+$ bacterial translocation and antitumor efficacy of CTX in *Nod1*$^{-/-}$*Nod2*$^{-/-}$ mice, we analyzed the role of individual NOD receptors in this potentiation. Conditional gene-deleted mice expressing a transgenic recombinase in intestinal epithelial cells under the control of a villin promoter with defective expression of NOD2 (*Nod2*$^{fl/fl}$ villin Cre$^+$) and NOD2-expressing wild-type (*Nod2*$^{fl/fl}$ villin Cre$^-$) were treated with tamoxifen and orally fed with *E. hirae* right before and after CTX administration prior to sacrifice to analyze the translocation of *E. hirae* in secondary lymphoid organs. The number of *E. hirae* colonies cultivable from mLN and spleens harvested from Cre$^+$ mice bearing NOD2 deficiency were markedly increased

compared with Cre- control mice (Figure 6A), indicating that intestinal NOD2 is a gate keeper normally preventing *E. hirae* translocation. The immune-dependent anti-sarcoma effects mediated by CTX were not ameliorated in *Nod1*$^{-/-}$, *Ripk2*$^{-/-}$, or *Card9*$^{-/-}$ mice compared with WT counterparts but were markedly enhanced in *Nod2*$^{-/-}$ mice (Figures 6B, S6A, and 6B). Accordingly, we phenocopied these effects using NOD2 receptor agonists, the peptidoglycans muramyl dipeptide inhibiting the antitumor effects of CTX in WT littermates (Figure S6C, left panel) while the TriDAP failed to have any effect (Figure S6C, right panel). Moreover, CTX-treated sarcoma growing in *Nod2*$^{-/-}$ mice contained fewer Treg cells (Figure 6C, left panels) and higher proportions of innate IFN-γ-producing γδTILs compared with sarcoma growing in WT counterparts (Figure 6C, right panels). These findings were reminiscent of the bioactivity observed with the "enforced" colonization by *E. hirae* and B. *intestinihominis*, respectively, in WT animals. To validate this assumption, we performed a gavage of *Nod2*$^{-/-}$ tumor-bearing mice with each OMB and monitored TILs by flow cytometry (Figure 6D). Both OMBs induced an increase in CD8$^+$ CTLs (Figure 6E, left panel), but *E. hirae* increased the CTL/Treg ratio

(Figure 6E, middle panel), whereas the *B. intestinihominis* augmented the proportion of γδTILs (Figure 6E, right panel) in *Nod2*$^{-/-}$ tumor-bearing mice.

To analyze the role of NOD2 receptors expressed by intestinal epithelial cells (IECs), we reduced the model system to crypt-derived 3D-small intestine enteroids generated from intestinal stem cells harvested from WT versus *Nod2*$^{-/-}$ mice (Vétizou et al., 2015). While short-term incubation of enteroids with mafosfamide (the active metabolite of the prodrug CTX) at the pharmacologically active concentration did not promote a NOD2-dependent apoptosis of IECs, *E. hirae* and *B. intestinihominis* rapidly induced cell demise of IECs, in a NOD2-dependent manner. Of note, *L. johnsonii* also induced IECs death independently of NOD2 (Figure 6F). Quantitative PCR analyses investigating the transcriptional oscillations of various gene products (IL-18, Bax, but not LysP and Grp78) involved in intestinal homeostasis corroborated the protective role of NOD2 receptors against the toxicity of these immunogenic bacteria (Figure 6G and data not shown) (Nigro et al., 2014).

Finally, conditional knockout mice expressing a transgenic recombinase in IECs under the control of a villin promoter with defective expression of NOD2 confirmed that IECs-associated NOD2 deficiency is necessary and sufficient to account for CTX-induced accumulation of pTh17 and γδT cells in the spleens (Figure 6H).

These findings suggest that IEC NOD2 receptors represent "gut immune checkpoints" restricting the immunogenicity of distinct Gram$^+$ and Gram$^-$ bacteria.

E. hirae- and *B. intestinihominis*- Specific Th1 Cell Immune Responses in Chemotherapy-Treated Cancer Patients

We analyzed the predictive value of preexisting memory CD4$^+$ CD45RO$^+$ Th1 immune responses directed against Gram$^+$ and Gram$^-$ bacteria for PFS in 38 advanced lung and ovarian cancer patients. PFS was analyzed regardless of subsequent therapies (Table S3). Culture supernatants of monocytes and memory CD4$^+$ T cells were monitored for IFN-γ and IL-10 secretion levels after restimulation with distinct commensals. Segregating the first cohort of lung cancers according to the median of IFN-γ produced by bacteria-specific memory T cells revealed that memory Th1 cells recognizing *E. hirae* and *B. intestinihominis* post-platinum based-chemotherapy predicted longer PFS, while Th1 cell recall responses toward other bacteria were not clinically relevant (Figures 7A and 7B and S7A). A second univariate analysis was performed by adding 13 advanced ovarian cancer patients resistant to platinum-based chemotherapy and treated with metronomic CTX. In this larger cohort, memory Th1 cells directed against *E. hirae* were the only protective T cell responses (Figure 7C). However, considering the ratio between IFN-γ and IL-10 release following stimulation, *B. intestinihominis* allowed to reach statistical significance for prolonged PFS in the whole cohort of advanced cancer patients (Figures 7D and 7E and S7B).

DISCUSSION

Here we identified key bacterial species involved in the immuno-modulatory effects of CTX, a major pillar of adjuvanticity used in a variety of immunotherapeutic protocols (Le et al., 2015; Lee et al., 2015; Sistigu et al., 2011). We showed that bacterial species belonging to two genera, *Enterococcus* and *Barnesiella*, were necessary and sufficient to mount effector and memory cancer-specific CD4$^+$ and CD8$^+$ T cells, thereby compensating for the loss or limited efficacy of CTX observed during ATBs-or cancer-induced dysbiosis, respectively.

The era of probiotics and microbiotherapy has come of age with the emergence of inflammatory disorders caused by an overt deviation of the gut microbiome (Cotillard et al., 2013; Kassam et al., 2013; Le Chatelier et al., 2013; Moayyedi et al., 2015). Although cancer-associated dysbiosis has not yet been characterized, one can anticipate that the host-microbe mutualism be disturbed in cancer bearers, for instance during chemotherapy-induced mucositis (Zitvogel et al., 2015), IEC-killing during CTLA4 blockade (Beck et al., 2006; Berman et al., 2010; Vétizou et al., 2015) or IEC damage and bacterial translocation during CTX therapy, exacerbated in the context of NOD2 deficiency as shown here. *E. hirae* was capable of decreasing Treg, γδT17 cells, and increased CD8$^+$ effector TILs, reinstating antitumor CTL activity). Most of the immunological (loss of DC and Th17 subsets) and inflammatory changes (increased proportions of Paneth cells) observed in the *lamina propria* (LP) during CTX metronomic therapy were observed in the small intestine, primarily in the duodenum and ileum (Viaud et al., 2013) which represent major colonization sites for enterococci (Ghosh et al., 2013). A high density of *E. hirae* (which tolerated gastric conditions and high bile salt concentrations) was found associated with a significant bactericidal effect against enteric pathogens (such as *Vibrio cholerae*, *E. faecalis*, *Enterobacter aerogenes*, *Pseudomonas aeruginosa*, *E. coli*, and *Salmonella* Typhi) (Arokiyaraj et al., 2014) and compete against *E. coli*, hereby preventing diarrhea in young kittens (Ghosh et al., 2013). The production of bacteriocins (such as hiracin JM79) by *E. hirae* facilitated the niche control in the intestine (Nes et al., 2014). However, the consequences of oral feeding with a commensal like *E. hirae* on the equilibrium of the small intestinal ecosystem remain to be elucidated.

Of interest, we found a Gram$^-$ bacterium ameliorating the effects of CTX, exerting different immunological effects on systemic and anticancer immune responses than *E. hirae*. Hence, sequencing analyses of feces from mice exhibiting a better response to CTX in the absence of NOD receptors highlighted the overrepresentation of the *Barnesiella* genus at the expense of *Lachnospiraceae* family members. The abundance of *Barnesiella* in the colon correlated with several other immunoregulatory cells such as marginal zone B cells and invariant NKT in the spleen and liver (Presley et al., 2010). The *Barnesiella* genus correlated with the clearance of vancomycin-resistant *Enterococcus faecium* in mice (Ubeda et al., 2013). In addition, *Barnesiella* densities were abnormally elevated in HIV-infected compared with non-infected individuals and associated with systemic inflammation (Dinh et al., 2015). Supporting this notion, *B. intestinihominis* was found overrepresented after ionizing radiation causing oxidative DNA damage, a therapeutic context where intestinal microbiota has a protective role (Maier et al., 2014). Here we describe the anticancer immunomodulatory role of *B. intestinihominis*. This Gram- bacterium markedly influenced the abundance of polyfunctional splenic Th1 and Tc1 cells and
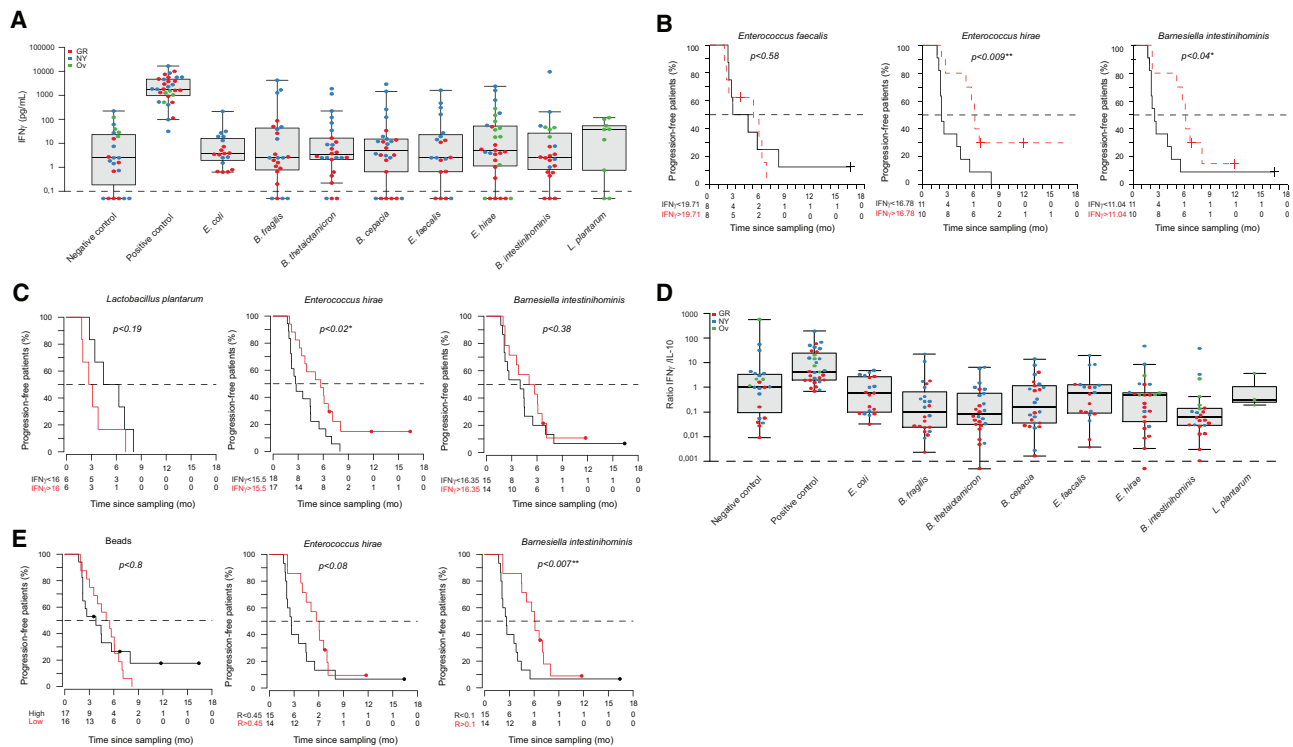
Figure 7. Memory Th1 Immune Responses to *E. hirae* and/or *B. intestinihominis* Associated with Prolonged PFS in Cancer Patients
(A) Raw data for 38 lung and ovarian cancer patients depicting the levels of IFN-γ release (and the mean) determined by ELISA for each patient prior to initiate immunotherapy after various bacterial stimulations of monocytes/CD4⁺CD45RO⁺ T cell cocultures. The univariate analyses and Kaplan Meier curves showing PFS for each subgroup of lung cancer patients above/below this mean are represented for each bacteria (B).
(C) Addition of 13 ovarian cancer patients to the lung cancer cohort to analyze the predictive value of *E. hirae*-specific Th1 immune responses for prolonged PFS.
(D) Raw data depicting ratio of IFN-γ/IL-10 determined by ELISA for each patient prior to initiate immunotherapy after various stimulations.
(E) Stratification according to the mean of the ratios of IFN-γ/IL-10 release in 38 patients. The univariate analyses and Kaplan Meier curves showing PFS for each subgroup of cancer patients above/below this mean ratio of IFN-γ/IL-10 are represented for *E. hirae* and *B. intestinihominis*. *p < 0.05, **p < 0.01. GR, Lung cancer treated with CTX-based vaccine; OV, Ovarian cancer on metronomic CTX; NY, Lung cancer on Ipilimumab combined with radiotherapy. Related to Figure S7 and Table S3.

increased the recruitment or proliferation of IFN-γ⁺ γδT cells in TILs, thereby behaving as OMBs with CTX against a wide spectrum of mouse cancers even in the absence of ATBs. The mechanism underlying these immune effects remain unclear, in that in contrast to *E. hirae*, *B. intestinihominis* failed to induce IL-12, IL-27, IL-1β, or Nos2 production by bone marrow DC in vitro.

What could be the mechanisms supporting why such commensals represent suitable OMBs? First, the geodistribution of such commensals might be crucial to enable access by intestinal phagocytes subsets to the immunogenic bacterium. Mucosal (as opposed to luminal) commensals or crypt-residing bacteria might be obvious candidates to regulate local and systemic immune responses (Farache et al., 2013; Palm et al., 2014; Pédron et al., 2012). Second, the deterministic model proposed by Littman and colleagues for Th cell differentiation in the intestine based on the bacterial context of cognate antigen delivery dictating the fate of antigen-specific T cells might hold true in our context, given the correlation between the capacity of clones of *E. hirae* to mount strong pTh17 immune responses and their OMB effect. *E. hirae* electively induced IL-6, IL-1β, and IL-23 in ex vivo propagated DC, cytokines involved in the pTh17 differentiation. Indeed, such an inflammatory or immunogenic profile of *E. hirae* 13144 ap-

peared highly protective in cancer patients. End-stage cancer patients resistant to platinum-based chemotherapy exhibited longer PFS when harboring prominent Th1 memory responses directed against *E. hirae* (or *B. intestinihominis*). Third, bacterial products might change the immunological tone of lymphoid organs (Ganal et al., 2012) or tumor beds (Iida et al., 2013), facilitating the elicitation of cancer antigen-specific T cells. Hence, Iida et al. exemplified that TLR4 was important for the efficacy of platinum salts in modulating intratumoral MDSC and inducing antitumor effects and demonstrated that LPS could partially compensate for the reduced tumoricidal activity of oxaliplatine in ATB-treated mice (Iida et al., 2013). Fourth, given that some bacteria (such as *E. hirae* and *B. intestinihominis)* are electively kept in check by NOD2 receptors, it is conceivable that loss-of-function mutations of NOD2 gene and impaired expression of NOD2 gate keepers in pathological circumstances will facilitate the elicitation of immune responses against these commensals/pathobionts. Fifth, bacteria-specific adaptive immune responses primed in mesenteric LN might express an array of chemokine receptors that dictate their homing to inflammatory lesions to reinstate local immunity (Bartman et al., 2015; Viaud et al., 2013). Hence, interruption of the CCR9/CCL25 axis promoted the growth of CCL25 producing

tumors by limiting the accumulation of CD4$^+$ Th cells in tumor draining lymph nodes (Jacquelot et al., 2016). Finally, a potential molecular mimicry between distinct commensals/pathobionts and tumor antigens is conceivable but remains to be established (Rubio-Godoy et al., 2002).

This study represents the rationale to reconstitute an optimal microbiota diversity integrating important species of the *Enterococcus* and *Barnesiella* genera to optimize the response to at least alkylating agents, currently employed in breast cancers, sarcomas, hematopoietic and pediatric malignancies. Altogether, these findings open the perspective of developing OMBs or their bacterial products (MAMPS or metabolites) to optimize cancer therapies (Zitvogel et al., 2015) and open the question as to whether any OMB could fit any cytotoxicant. We surmise that the near future will undoubtedly unravel new OMBs suitable for other therapeutic compounds with their peculiar mode of action.

EXPERIMENTAL PROCEDURES

Mice
All animal experiments were carried out in compliance with the French and European laws and regulations. Mice were used between 7 and 16 weeks of age. WT specific pathogen-free C57BL/6J mice were obtained from Harlan (France) and were kept in SPF conditions in the animal facility of Gustave Roussy, Villejuif, France. *Nod1*$^{-/-}$, *Nod2*$^{-/-}$, and *Nod1*$^{-/-}$*Nod2*$^{-/-}$ C57BL/6J mice were kindly provided by I. Gomperts Boneca (Institut Pasteur, Paris), *Nod2 Villin-cre* and *Ripk2*$^{-/-}$ C57BL/6J by M. Chamaillard (Institut Pasteur, Lille), and *Card9*$^{-/-}$ C57BL/6J by H. Sokol (Hôpital Saint Antoine, Paris). Mice were maintained in sterile isolators.

Tumor Challenge and Treatment
0.8–1 × 10^6 MCA205, MC38-OVA^{dim}, MCA205-OVA, or 0.5 × 10^6 TC-1 and Ret tumor cells were inoculated subcutaneously in the right flank. When tumors reached a size of 20 to 40 mm^2 (day 0), mice were injected weekly i.p with 100 mg/kg of cyclophosphamide (CTX, Endoxan, Baxter provided by GRCC) or NaCl. For tumor rechallenge in the settings of OVA vaccination, mice were inoculated with 3 × 10^6 MC38-OVA^{dim}. Tumor size was routinely monitored by means of a caliper. In villin-Cre-conditional KO mice experiments, tamoxifen was provided by CM. Mice were injected i.p. with 50 mg/kg of tamoxifen 1 month before use. MDP and TriDAP (Invivogen) were injected i.p., at a dose of 100 μg per mouse. Neutralization experiments: In experiments using anti-IL-17 (clone 17F3, 200 μg per mouse) or anti-IFN-γ (clone R4-6A2, 200 μg per mouse) mAb, antibodies (or their isotype controls (MOPC-21 or HRPN, respectively)) were injected i.p. twice a week from the beginning of the experiment until the final injection of cyclophosphamide. In order to deplete CD8$^+$ T cells, clone 53-6.72 (200 μg per mouse) or isotype control 2A3 were injected i.p. twice a week from the beginning of the experiment until the final injection of cyclophosphamide. All mAb were obtained from BioXcell (West Lebanon, NH, USA).

Gut Colonization with Dedicated Bacterial Species
Colonization of ATBs pre-treated or naive C57BL/6 mice was performed by oral gavage with 100 μl of suspension containing 1 × 10^9 bacteria. Efficient colonization was confirmed by culture of feces 48 hr post-gavage. Fecal pellet contents were harvested and resuspended in BHI+15% glycerol at 0.1 g/ml. Serial dilutions of feces were plated onto sheep's blood agar plates (COS, Biomérieux) and incubated for 48h at 37°C with 5% CO$_2$ in aerobic or anaerobic conditions. After 48 hr, single colonies were isolated and Gram staining was performed. The identification of specific bacteria was accomplished through the combination of morphological tests and analysis by means of an Andromas MALDI-TOF mass spectrometer (Andromas, France). *Barnesiella intestinihominis* was kindly provided by D.R. *E. coli* MC1061, *E. faecalis* JH2-2 and *L. plantarum* NCIMB8826 were kindly provided by I.G.B. *Lactobacillus johnsonii* and *Enterococcus hirae* isolates used in the experiments were originally isolated from spleens or mesenteric lymph nodes of SPF mice treated with CTX.

Alternate *E. hirae* isolates were provided by V.C. *Lactobacillus plantarum*, *Lactobacillus johnsonii*, *Enterococcus hirae*, *Enterococcus faecalis* JH2-2, and *Barnesiella intestinihominis* were all grown on COS plates for 48 hr at 37°C in anaerobic conditions. *Escherichia coli* was grown on COS plates for 24h at 37°C in aerobic conditions. Bacteria were harvested from the agar plates, suspended in sterile NaCl at an optical density (600 nm) of 1, which corresponds approximately to 1 × 10^9 colony-forming units (CFU)/ml, centrifuged, washed once, and then resuspended in sterile NaCl. For bacteria reconstitution experiments using mice previously treated with ATBs, ATBs treatment was stopped after 2 weeks, mice were then treated with CTX and were orally gavaged with 1 × 10^9 CFU the following day. For bacteria reconstitution experiments using mice not-treated with ATBs, mice were orally gavaged with 1 × 10^9 CFU and treated with CTX the following day.

SUPPLEMENTAL INFORMATION

Supplemental Information includes six figures, three tables, and Supplemental Experimental Procedures and can be found with this article online at http://dx.doi.org/10.1016/j.immuni.2016.09.009.

AUTHOR CONTRIBUTIONS

L.Z. conceived the study, analyzed the data, provided the intellectual guidance, and wrote the paper with G.K.'s editing. R.D., M.V., N.J., T.Y., B.R., S.R., C.F., N.W., M.P.R., C.P.M.D., S.B., V.P.-C., V.C., L.A., and C.I. performed experiments and analyzed data. D.E. and P.L. analyzed bioinformatics data. D.R., M.C., I.G.B., P.L., H.S., V.C., and E.T. provided mice, bacteria, and reagents. A.E., E.C., P.-L.W., M.C., V.C., and I.G.B. also provided intellectual guidance. M.P., M.M., J.-C.S., E.G., S.F. were in charge of patients enrollment for clinical trials.

REFERENCES

Arokiyaraj, S., Hairul Islam, V.I., Bharanidharan, R., Raveendar, S., Lee, J., Kim, D.H., Oh, Y.K., Kim, E.-K., and Kim, K.H. (2014). Antibacterial,

anti-inflammatory and probiotic potential of Enterococcus hirae isolated from the rumen of Bos primigenius. World J. Microbiol. Biotechnol. 30, 2111–2118.

Bartman, C., Chong, A.S., and Alegre, M.-L. (2015). The influence of the microbiota on the immune response to transplantation. Curr. Opin. Organ Transplant. 20, 1–7.

Beck, K.E., Blansfield, J.A., Tran, K.Q., Feldman, A.L., Hughes, M.S., Royal, R.E., Kammula, U.S., Topalian, S.L., Sherry, R.M., Kleiner, D., et al. (2006). Enterocolitis in patients with cancer after antibody blockade of cytotoxic T-lymphocyte-associated antigen 4. J. Clin. Oncol. 24, 2283–2289.

Berman, D., Parker, S.M., Siegel, J., Chasalow, S.D., Weber, J., Galbraith, S., Targan, S.R., and Wang, H.L. (2010). Blockade of cytotoxic T-lymphocyte antigen-4 by ipilimumab results in dysregulation of gastrointestinal immunity in patients with advanced melanoma. Cancer Immun. 10, 11.

Blaser, M. (2011). Antibiotic overuse: Stop the killing of beneficial bacteria. Nature 476, 393–394.

Cotillard, A., Kennedy, S.P., Kong, L.C., Prifti, E., Pons, N., Le Chatelier, E., Almeida, M., Quinquis, B., Levenez, F., Galleron, N., et al.; ANR MicroObes consortium (2013). Dietary intervention impact on gut microbial gene richness. Nature 500, 585–588.

Dinh, D.M., Volpe, G.E., Duffalo, C., Bhalchandra, S., Tai, A.K., Kane, A.V., Wanke, C.A., and Ward, H.D. (2015). Intestinal microbiota, microbial translocation, and systemic inflammation in chronic HIV infection. J. Infect. Dis. 211, 19–27.

Farache, J., Zigmond, E., Shakhar, G., and Jung, S. (2013). Contributions of dendritic cells and macrophages to intestinal homeostasis and immune defense. Immunol. Cell Biol. 91, 232–239.

Ganal, S.C., Sanos, S.L., Kallfass, C., Oberle, K., Johner, C., Kirschning, C., Lienenklaus, S., Weiss, S., Staeheli, P., Aichele, P., and Diefenbach, A. (2012). Priming of natural killer cells by nonmucosal mononuclear phagocytes requires instructive signals from commensal microbiota. Immunity 37, 171–186.

Ghosh, A., Borst, L., Stauffer, S.H., Suyemoto, M., Moisan, P., Zurek, L., and Gookin, J.L. (2013). Mortality in kittens is associated with a shift in ileum mucosa-associated enterococci from Enterococcus hirae to biofilm-forming Enterococcus faecalis and adherent Escherichia coli. J. Clin. Microbiol. 51, 3567–3578.

Gur, C., Ibrahim, Y., Isaacson, B., Yamin, R., Abed, J., Gamliel, M., Enk, J., Bar-On, Y., Stanietsky-Kaynan, N., Coppenhagen-Glazer, S., et al. (2015). Binding of the Fap2 protein of Fusobacterium nucleatum to human inhibitory receptor TIGIT protects tumors from immune cell attack. Immunity 42, 344–355.

Iida, N., Dzutsev, A., Stewart, C.A., Smith, L., Bouladoux, N., Weingarten, R.A., Molina, D.A., Salcedo, R., Back, T., Cramer, S., et al. (2013). Commensal bacteria control cancer response to therapy by modulating the tumor microenvironment. Science 342, 967–970.

Jacquelot, N., Enot, D.P., Flament, C., Vimond, N., Blattner, C., Pitt, J.M., Yamazaki, T., Roberti, M.P., Daillère, R., Vétizou, M., et al. (2016). Chemokine receptor patterns in lymphocytes mirror metastatic spreading in melanoma. J. Clin. Invest. 126, 921–937.

Kassam, Z., Lee, C.H., Yuan, Y., and Hunt, R.H. (2013). Fecal microbiota transplantation for Clostridium difficile infection: systematic review and meta-analysis. Am. J. Gastroenterol. 108, 500–508.

Le, D.T., Wang-Gillam, A., Picozzi, V., Greten, T.F., Crocenzi, T., Springett, G., Morse, M., Zeh, H., Cohen, D., Fine, R.L., et al. (2015). Safety and survival with GVAX pancreas prime and Listeria Monocytogenes-expressing mesothelin (CRS-207) boost vaccines for metastatic pancreatic cancer. J. Clin. Oncol. 33, 1325–1333.

Le Chatelier, E., Nielsen, T., Qin, J., Prifti, E., Hildebrand, F., Falony, G., Almeida, M., Arumugam, M., Batto, J.-M., Kennedy, S., et al.; MetaHIT consortium (2013). Richness of human gut microbiome correlates with metabolic markers. Nature 500, 541–546.

Lee, D.W., Kochenderfer, J.N., Stetler-Stevenson, M., Cui, Y.K., Delbrook, C., Feldman, S.A., Fry, T.J., Orentas, R., Sabatino, M., Shah, N.N., et al. (2015). T cells expressing CD19 chimeric antigen receptors for acute lymphoblastic leukaemia in children and young adults: a phase 1 dose-escalation trial. Lancet 385, 517–528.

Louis, P., Hold, G.L., and Flint, H.J. (2014). The gut microbiota, bacterial metabolites and colorectal cancer. Nat. Rev. Microbiol. 12, 661–672.

Maier, I., Berry, D.M., and Schiestl, R.H. (2014). Intestinal microbiota reduces genotoxic endpoints induced by high-energy protons. Radiat. Res. 181, 45–53.

Moayyedi, P., Surette, M.G., Kim, P.T., Libertucci, J., Wolfe, M., Onischi, C., Armstrong, D., Marshall, J.K., Kassam, Z., Reinisch, W., and Lee, C.H. (2015). Fecal Microbiota Transplantation Induces Remission in Patients With Active Ulcerative Colitis in a Randomized Controlled Trial. Gastroenterology 149, 102–109.e6.

Nes, I.F., Diep, D.B., and Ike, Y. (2014). Enterococcal Bacteriocins and Antimicrobial Proteins that Contribute to Niche Control. In Enterococci: From Commensals to Leading Causes of Drug Resistant Infection, M.S. Gilmore, D.B. Clewell, Y. Ike, and N. Shankar, eds. (Boston: Massachusetts Eye and Ear Infirmary).

Nigro, G., Rossi, R., Commere, P.-H., Jay, P., and Sansonetti, P.J. (2014). The cytosolic bacterial peptidoglycan sensor Nod2 affords stem cell protection and links microbes to gut epithelial regeneration. Cell Host Microbe 15, 792–798.

Palm, N.W., de Zoete, M.R., Cullen, T.W., Barry, N.A., Stefanowski, J., Hao, L., Degnan, P.H., Hu, J., Peter, I., Zhang, W., et al. (2014). Immunoglobulin A coating identifies colitogenic bacteria in inflammatory bowel disease. Cell 158, 1000–1010.

Paulos, C.M., Wrzesinski, C., Kaiser, A., Hinrichs, C.S., Chieppa, M., Cassard, L., Palmer, D.C., Boni, A., Muranski, P., Yu, Z., et al. (2007). Microbial translocation augments the function of adoptively transferred self/tumor-specific CD8+ T cells via TLR4 signaling. J. Clin. Invest. 117, 2197–2204.

Pédron, T., Mulet, C., Dauga, C., Frangeul, L., Chervaux, C., Grompone, G., and Sansonetti, P.J. (2012). A crypt-specific core microbiota resides in the mouse colon. MBio 3, 3.

Presley, L.L., Wei, B., Braun, J., and Borneman, J. (2010). Bacteria associated with immunoregulatory cells in mice. Appl. Environ. Microbiol. 76, 936–941.

Rossini, A., Rumio, C., Sfondrini, L., Tagliabue, E., Morelli, D., Miceli, R., Mariani, L., Palazzo, M., Ménard, S., and Balsari, A. (2006). Influence of antibiotic treatment on breast carcinoma development in proto-neu transgenic mice. Cancer Res. 66, 6219–6224.

Rubio-Godoy, V., Dutoit, V., Zhao, Y., Simon, R., Guillaume, P., Houghten, R., Romero, P., Cerottini, J.-C., Pinilla, C., and Valmori, D. (2002). Positional scanning-synthetic peptide library-based analysis of self- and pathogen-derived peptide cross-reactivity with tumor-reactive Melan-A-specific CTL. J. Immunol. 169, 5696–5707.

Rutkowski, M.R., Stephen, T.L., Svoronos, N., Allegrezza, M.J., Tesone, A.J., Perales-Puchalt, A., Brencicova, E., Escovar-Fadul, X., Nguyen, J.M., Cadungog, M.G., et al. (2015). Microbially driven TLR5-dependent signaling governs distal malignant progression through tumor-promoting inflammation. Cancer Cell 27, 27–40.

Sandoval, F., Terme, M., Nizard, M., Badoual, C., Bureau, M.F., Freyburger, L., Clement, O., Marcheteau, E., Gey, A., Fraisse, G., et al. (2013). Mucosal imprinting of vaccine-induced CD8+ T cells is crucial to inhibit the growth of mucosal tumors. Sci. Transl. Med. 5, 172ra20.

Sears, C.L., and Garrett, W.S. (2014). Microbes, microbiota, and colon cancer. Cell Host Microbe 15, 317–328.

Sistigu, A., Viaud, S., Chaput, N., Bracci, L., Proietti, E., and Zitvogel, L. (2011). Immunomodulatory effects of cyclophosphamide and implementations for vaccine design. Semin. Immunopathol. 33, 369–383.

Sivan, A., Corrales, L., Hubert, N., Williams, J.B., Aquino-Michaels, K., Earley, Z.M., Benyamin, F.W., Lei, Y.M., Jabri, B., Alegre, M.-L., et al. (2015). Commensal Bifidobacterium promotes antitumor immunity and facilitates anti-PD-L1 efficacy. Science 350, 1084–1089.

Ubeda, C., Bucci, V., Caballero, S., Djukovic, A., Toussaint, N.C., Equinda, M., Lipuma, L., Ling, L., Gobourne, A., No, D., et al. (2013). Intestinal microbiota containing Barnesiella species cures vancomycin-resistant Enterococcus faecium colonization. Infect. Immun. 81, 965–973.

Velicer, C.M., Heckbert, S.R., Lampe, J.W., Potter, J.D., Robertson, C.A., and Taplin, S.H. (2004). Antibiotic use in relation to the risk of breast cancer. JAMA *291*, 827–835.

Vétizou, M., Pitt, J.M., Daillère, R., Lepage, P., Waldschmitt, N., Flament, C., Rusakiewicz, S., Routy, B., Roberti, M.P., Duong, C.P.M., et al. (2015). Anticancer immunotherapy by CTLA-4 blockade relies on the gut microbiota. Science *350*, 1079–1084.

Viaud, S., Saccheri, F., Mignot, G., Yamazaki, T., Daillère, R., Hannani, D., Enot, D.P., Pfirschke, C., Engblom, C., Pittet, M.J., et al. (2013). The intestinal microbiota modulates the anticancer immune effects of cyclophosphamide. Science *342*, 971–976.

Vingert, B., Adotevi, O., Patin, D., Jung, S., Shrikant, P., Freyburger, L., Eppolito, C., Sapoznikov, A., Amessou, M., Quintin-Colonna, F., et al. (2006). The Shiga toxin B-subunit targets antigen in vivo to dendritic cells and elicits anti-tumor immunity. Eur. J. Immunol. *36*, 1124–1135.

Zitvogel, L., Galluzzi, L., Viaud, S., Vétizou, M., Daillère, R., Merad, M., and Kroemer, G. (2015). Cancer and the gut microbiota: an unexpected link. Sci. Transl. Med. *7*, 271ps1.